Chitosan−SDS Interactions at a Solid−Liquid Interface: Effects of Surfactant Concentration and Ionic Strength†

Andra Dėdinaitė*,‡ and Marie Ernstsson§

Unilever Research and Development Port Sunlight, Quarry Road East, Bebington, Wirral CH63 3JW, United Kingdom and Institute for Surface Chemistry, Box 5607, SE−114 86 Stockholm, Sweden

Received: November 27, 2002; In Final Form: May 12, 2003

The effect of ionic strength on adsorption of chitosan on mica as well as the impact of addition of an anionic surfactant, SDS, on the adsorbed chitosan layers is explored. It is demonstrated by chemical surface analysis (ESCA) and surface force measurements (SFA) that an elevated salt concentration leads to larger adsorbed amounts and thicker adsorption layers of this cationic polyelectrolyte. It is also shown that in contrast to the bulk, the binding of oppositely charged surfactant to the polyelectrolyte adsorbed on a negatively charged surface is facilitated by elevated ionic strength. Thus, the association process in bulk and at solid−liquid interfaces is rather different. The main point of difference is that at the solid−liquid interface one also has to consider interactions between the polyelectrolyte and the surface as well as between the surfactant and the surface.

Introduction

The need for a better understanding of chitosan adsorption and interactions between chitosan adsorption layers and surfactants becomes evident in the context of the desire to more efficiently utilize this easily available biopolymer. Chitosan is obtained by N-deacetylation of chitin, the next most abundant natural polysaccharide after cellulose.[1] It is an invaluable renewable natural resource whose technological importance is becoming increasingly evident. Numerous reports on the applications of chitosan, ranging from wastewater treatment[2] to biomedical and pharmaceutical applications such as, e.g., cancer treatment, wound dressing, contact lenses or controlled drug release,[1,3] can be found in the literature. In many of these applications chitosan is extremely attractive due to its biocompatibility, biodegradability, and nontoxicity[1−3] along with its fungistatic and antibacterial activity.[2−8]

With the above in mind, it is surprising that only a few fundamental studies exploring the adsorption properties of chitosan have been carried out. In one such study Domard et al.[9] investigated the adsorption of chitosan and its quaternized derivative on kaolin, possessing a negative charge at pH values above 4. It was found that the level of the adsorption plateau of the quaternized chitosan derivative decreases with a decrease in pH due to the decreased charge density of the kaolin substrate and the increased linear charge density of chitosan. The role of the pH is even more pronounced for the unmodified chitosan—the adsorption plateau cannot be attained at pH 6, which presumably is due to the poor solubility of chitosan at high pH. Despite an obvious need to understand adsorption and the forces generated by chitosan adsorption layers, the number of studies investigating this topic is small.[10,11] Most exploratory among these is one by Claeson and Ninham.[12] By using chitosan with a degree of deacetylation of 90−95%, these authors demonstrated that adsorption of chitosan on mica surfaces results in a flat adsorbed layer and a reversal of the sign of the surface charge at low pH. The adsorption is essentially irreversible with respect to dilution and pH changes. However, the surface interactions and the structure of adsorbed layers depend considerably on the pH. These changes are reversible. The results reported in the literature point to the possibility of using chitosan for surface coating and modification purposes.

In the context of surface conditioning by using polymers, an important issue is their interactions with surface-active materials. In previous work carried out in our research groups, employing copolymers of a charged monomer and acrylamide, we showed that addition of surfactants to preadsorbed polyelectrolyte layers has a dramatic effect on the adsorbed layer structure and, consequently, on the interaction forces. Surface force measurements demonstrated that surfactant addition may induce periodic layer structures,[13] strong swelling,[14,15] or desorption,[16] depending on polyelectrolyte charge density and surfactant concentration. The change in adsorbed amount of polyelectrolyte due to exposure of the preadsorbed polyelectrolyte layer has been followed by XPS.[17] Recently, the swelling of preadsorbed polyelectrolyte layers induced by surfactant addition has also been followed using the quartz crystal microbalance technique.[18] This work puts an emphasis on chitosan−surfactant interaction at the solid−liquid interface. The effect of ionic strength on adsorption of chitosan on mica as well as the impact of addition of an anionic surfactant, SDS, on the adsorbed chitosan layers are studied. We combined information obtained by surface force measurements, which allow us to explore how the polymer layers change due to changes in solution composition, with results from ESCA measurements, which provide chemical information and allow quantification of the adsorbed amount.

Experimental Section

Solution Preparation. Chitosan with a molecular weight of 150 000 g/mol and deacetylation degree of 84.5%, containing ≤1% of insoluble matter, was obtained from Fluka (Cat. No. 22741). Chitosan to a concentration of 1% w/v was dispersed

† Part of the special issue "International Synmposium on Polyelectrolytes".

‡ Present address: Department of Chemistry, Surface Chemistry, Royal Institute of Technology, SE-100 44 Stockholm, Sweden.

§ Institute for Surface Chemistry.

10.1021/jp027571t CCC: $25.00
Published on Web 06/21/2003

in 1% aqueous glacial acetic acid (Merck, pro analysi grade) solution. To achieve a complete dissolution of all soluble material, chitosan was left mixing for 48 h. Prior to injecting the chitosan solution between the mica surfaces, it was diluted to 20 ppm using a $NaNO_3$ solution of an appropriate concentration. SDS was purchased from Sigma (Cat. No. L4509) and further purified by recrystalization from Milli Q water, repeating the procedure twice. The water used for solution preparation was first treated with a Milli-RO 10 Plus unit including depth filtration, carbon adsorption, and decalcination preceding reverse osmosis. Further, the water was passed through a Milli-Q plus 185 purification unit.

Bulk Studies. The turbidity of chitosan−SDS mixtures containing 20 ppm chitosan and SDS in the concentration range 0−1 cmc in 30 mM NaCl solution was measured employing a turbidimeter C114, Hanna instruments, Portugal. Individual samples for each SDS concentration were prepared rather than increasing the SDS concentration in a stepwise manner. The turbidity was measured 15 min after the mixing of the components.

Chemical Surface Analysis. The adsorbed amount of chitosan on mica surfaces after exposure to a range of SDS solutions in the concentration range (0−1 cmc) was quantified utilizing ESCA spectra recorded using a Kratos AXIS HS X-ray photoelectron spectrometer (Kratos Analytical, Manchester, UK). The cmc of SDS in 30 and 0.1 mM NaCl is 3.2 and 8.3 mM, respectively. The samples were analyzed using two modes of operation, referred to as Al-*elstat* and Al-*mono*. In the Al-*elstat* mode, unmonochromatized Al X-rays from a dual anode irradiate the sample and the electrostatic lens is used to collect photoelectrons from a relatively large sample area (order of 1 cm^2). Due to the large area analyzed and the short distance between anode and sample, this mode gives rather high signal intensities. In the Al-*mono* mode, using monochromatized Al X-rays and the so-called slotM (magnetic) lens, the analyzed area is less than 1 mm^2. The small area analyzed together with the much larger distance between anode and sample give lower signal intensities in the Al-*mono* mode. However, the great advantage using the monochromator is that the peak widths are reduced, providing the possibility of separating peaks in high-resolution spectra. For further details, readers are referred to the work of Rojas et al.[19]

In the current work we adopted the method of Rojas et al.[19] to quantify the adsorption of chitosan on mica. The adsorbed amount is determined from comparison between the nitrogen 1s peak emanating from the polyelectrolyte and the potassium 2p peak from the mica substrate. Since the number of exchangeable potassium ions on the mica surface is known (2.1×10^{18} surface lattice sites/m^2), the quantification procedure is relatively straightforward.

To provide a good comparison between the SFA and the ESCA results, nearly identical surface preparation procedures were used. Mica surfaces employed for ESCA analysis were freshly cleaved in a laminar flow hood and cut into pieces with dimensions of 2×4 cm. To reduce any contamination of the high-energy mica surface, the mica slabs were immersed into the aqueous 20 ppm chitosan solutions containing either 0.1 or 30 mM NaCl immediately after cleaving. Adsorption was allowed for 60 min. It was followed by immersion for 30 min in a chitosan-free solution of the same ionic strength. Thereafter, the mica slabs were transferred into beakers containing solutions of SDS with appropriate SDS concentration where they were allowed to stand for 60 min. Finally, each surface was dipped in the respective NaCl solution (containing no polymer or surfactant) for 10 min and then gently blown dry with a filtered nitrogen jet. To avoid unwanted Langmuir−Blodgett deposition of surface-active contaminants, the water surface was cleaned by suction using a Pasteur pipet connected to a water vacuum pump immediately before each transfer of the surface through the tree phase line.

Surface Force Measurements. Forces between chitosan adsorption layers on mica surfaces were measured by using the interferometric surface force apparatus (SFA) employing the Mark IV[20] model. The basic principles behind this technique and a detailed description of its function are given elsewhere.[21,22] In brief, the two molecularly smooth mica sheets are silvered on one side with the silvered side glued down onto optically polished semicylindrical silica disks. White light is shone via the window positioned in the bottom of the apparatus and multiply reflected between the silver layers. Fringes of equal chromatic order (FECO) created during the constructive interference pass through the upper silver layer and are directed to the spectrometer. From the wavelengths of FECO when the two mica surfaces are in direct contact and some distance apart, the separation between the surfaces can be measured with an accuracy of 0.1 nm. The force is determined by changing the distance between the surfaces using either a synchronous motor or a piezoelectric crystal tube and subsequently measuring the actual surface motion. The difference between the expected and the real shift in separation when multiplied by the spring constant of the force measuring spring gives the difference in force between the two positions. The local geometric mean radius, R, is approximately 2 cm, but it varies somewhat between different experiments. To relate data obtained in different experiments, the force, F, is normalized by the radius, R, and according to the Derjaguin approximation,[23] this is related to the free energy of interaction per unit area between flat surfaces $G_f(D)$

$$\frac{F(D)}{R} = 2\pi G_f(D) \tag{1}$$

This relation is valid provided $R \gg D$. As the range of the interaction in our experiments is on the order of 10^{-6} m or less, the latter condition is always satisfied. Another requirement is that the radius of the surfaces should be independent of surface separation. This is not the case when very strong attractive or repulsive forces are in action, causing deformation of the surfaces.[24] When the force gradient $\partial F/\partial D$ exceeds the spring constant, the mechanical force measuring system becomes unstable and the surfaces jump together or apart to another stable force−distance region.

In one set of experiments we probed the interactions between mica sheets by inserting a 60 μL droplet of 20 ppm chitosan solution in 0.1 or 30 mM $NaNO_3$ (pH ~4) between the surfaces. To ascertain that the concentration of components present in the droplet did not change due to evaporation, a beaker containing a solution of identical composition to that of the droplet was placed within the closed chamber of the SFA. In another set of experiments, chitosan was allowed to adsorb on mica for 60 min from a 20 ppm chitosan solution in 0.1 or 30 mM $NaNO_3$ outside of the SFA. Next, the surfaces were rinsed in a chitosan-free $NaNO_3$ solution of respective concentration for 10 min in order to remove all nonadsorbed chitosan. After this the surfaces were immediately mounted in the SFA in order to avoid drying of the adsorbed layer. Initially, the chamber was filled with 0.1 or 30 mM $NaNO_3$ solution (pH ~ 6). Subsequently, to study association between adsorbed chitosan

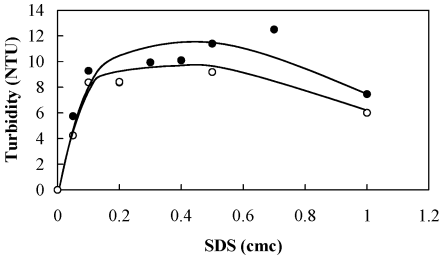

Figure 1. Turbidity in 20 ppm chitosan solutions in 30 mM NaCl pH 6 (○) and pH 4 (●) as a function of SDS concentration 15 min after mixing.

and the anionic surfactant, SDS, the surfactant was injected to an appropriate concentration in the range from 0 to 1 cmc.

Results

Bulk Properties of Chitosan−SDS Solutions. The turbidity of chitosan−SDS mixtures in 30 mM NaCl solution at pH 4 and 6 after 15 min of mixing is shown in Figure 1.

As seen in Figure 1, the turbidity of the solution increases already at a rather low SDS concentration (<0.1 cmc). This demonstrates that the association of chitosan and SDS has proceeded sufficiently to allow formation of large aggregates in the solution. The turbidity remains high at higher SDS concentrations even though a slight decrease can be seen at cmc. The turbidity at pH 4 is somewhat higher as compared to pH 6, which presumably is related to the higher charge density of chitosan at the lower pH value, which results in a stronger association with the anionic surfactant. We note that in the SDS concentration 0.05−0.6 cmc the aggregates flocculate with time and a precipitate forms. At higher SDS concentrations, the dispersed aggregates are stable, indicating a recharging.

Chemical Surface Analysis. Adsorption of chitosan produces a distinctive N 1s peak in the ESCA spectrum. This peak originates from the nitrogen atoms in the polyelectrolyte. In addition, the C 1s signal increases. Some typical detailed N 1s spectra are shown in Figure 2.

The nitrogen 1s signal arising from uncharged amine appears as a peak at a binding energy of about 400 eV.[19,25] In an ammonium salt the peak is shifted toward higher binding energy (ca. 402−403 eV).[19,25] After performing curve fitting, it was found that in our case the two N 1s peaks are separated by 2.3−2.6 eV.

As seen in Figure 3, for adsorbed layers formed from solutions containing high salt concentration (30 mM), most of the nitrogen signal arises from the uncharged (60−66%) nitrogen. In contrast, for adsorbed chitosan layers formed from low salt concentration solutions (0.1 mM), most nitrogen in the adsorbed layer is charged (50−62% of total signal; see also the curve fitted N 1s spectra in Figure 2 a−c).

Table 1 shows the adsorbed amount calculated according to eq 12 in the work by Rojas et al.[19]

The columns in Table 1 show the adsorbed amount using Al-*mono* values direct, Al-*elstat* values direct, and Al-*elstat* values with an adjusted baseline. The location of the baselines can be seen in Figure 4 a−c.

The adjustment of the baseline for the K 2p peak was done since the K 2p and C 1s peaks are not fully separated in the Al-*elstat* mode (Figure 4b), leading to an underestimation of the K 2p raw areas, which gives an overestimation of the calculated adsorbed amounts. The trend with a higher deduced adsorbed amount for Al-*elstat* than for Al-*mono* have been observed previously (see, e.g., Rojas et al.[19]) but not fully understood. The results presented in the current paper resolves the issue, and it is clear that adsorbed amounts obtained using

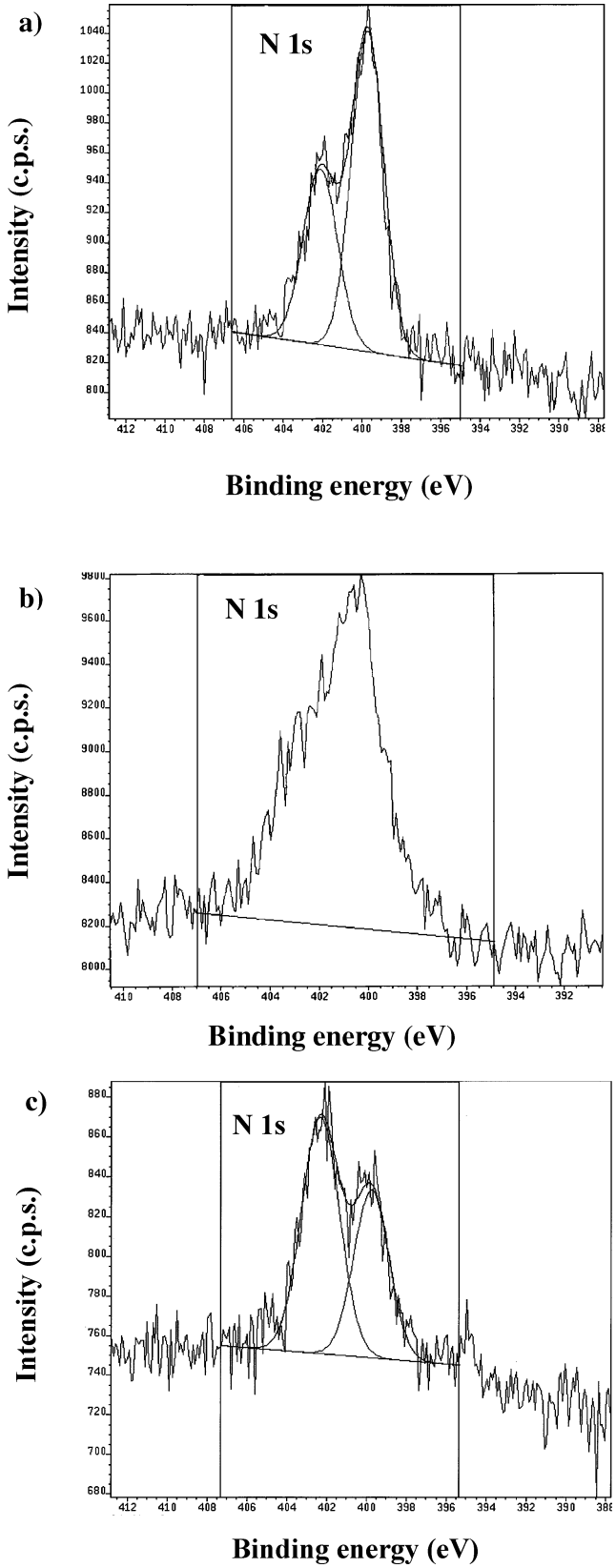

Figure 2. Nitrogen 1s spectra for chitosan exposed to 0.5 cmc SDS solution in 30 mM NaCl (a) Al-*mono* and (b) Al-*elstat* mode and in 0.1 mM NaCl solution Al-*mono* (c).

the Al-*mono* mode are most correct. Further, we demonstrate that the Al-*elstat* mode can be used with better accuracy provided a baseline correction for the K 2p peak is implemented, as demonstrated in Figure 4c. We note that a (smaller) discrepancy between the Al-*mono* mode and the Al-*elstat* mode

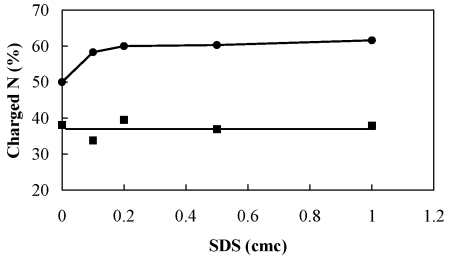

Figure 3. Percentage of the nitrogen peak due to the presence of charged nitrogen as a function of SDS concentration in 0.1 mM NaCl (●) and 30 mM NaCl (■). Calculated from the spectra obtained using the Al-*mono* mode.

remains also after the baseline correction has been carried out. One reason for this is the difficulty of performing this correction in an accurate way.

The results in Table 1 clearly show that more chitosan is adsorbed from 30 mM NaCl than from the 0.1 mM solutions and though the role of electrostatic forces is of clear importance, there also exist nonelectrostatic factors that play a role in the adsorption process.[26,27] Further, hardly any desorption occurs upon exposing the preadsorbed chitosan layer to SDS solutions up to a concentration corresponding to the cmc of the surfactant.

Surface Interactions in 0.1 mM $NaNO_3$. Interactions between mica surfaces across the droplet containing 20 ppm chitosan in 0.1 mM $NaNO_3$ are shown in Figure 5.

There is no electrical double-layer force present. This shows that mica with the adsorbed chitosan layer carries a 0 net charge. A strong attractive force pulls the surfaces together from a separation of about 11 nm and brings them into a separation of about 1.3 nm. The jump occurs when the gradient of the force just exceeds the spring constant of the force measuring spring. The jump distance due to van der Waals forces is expected to be in the range of 12−11 nm. This agrees very nicely with the jump distance measured experimentally (Figure 5). However, once the surfaces are in contact, some interchange of the adsorbed polymer segments between the surfaces is possible. Thus, during separation, the attraction is due to two components, a van der Waals attraction and an attraction due to bridging of the polyelectrolyte chains attached to the opposite surfaces. The bridging force has been observed previously in systems containing highly positively charged polyelectrolytes adsorbed on highly negatively charged surfaces[13] and the origin of it was explained.[28] Due to the attractive force a subsequent flattening of the polyelectrolyte adsorption layers to 1 nm takes place. The thickness is in good agreement with that measured for other highly charged polylelectrolytes[13,28] and in accordance with the thin compressed layer of 1.5 nm measured for chitosan adsorbed on mica from 0.01% (100 ppm) solution.[12] When the surfaces were separated, an attractive minimum of 2 ± 0.8 mN/m was detected at a separation of 2.7−3.2 nm. We note the increase in distance during separation. It indicates the stretching of adsorbed polymer chains between the surfaces. Both the low pull-off force, compared to what has been found for mica coated with other highly charged polyelectrolytes,[13,29] and the gradual increase in separation are in line with previously reported results for chitosan−mica systems under different conditions.[12]

Dilution of the 20 ppm 60 μL droplet with 400 mL of 0.1 mM $NaNO_3$ results in a chitosan bulk concentration of 3 ppb and brings the pH of the solution to close to 6. Due to the increase in pH, the charge of chitosan is bound to decrease. In fact, at this pH the charge of chitosan is nearly halved as compared to the charge at pH 4 (pK_a of chitosan is around 6.6).[30−32] Even so, as evidenced by the measured surface interactions at these conditions (Figure 5), the dilution did not lead to any considerable chitosan desorption from the surface, which is related to the high polymer surface affinity and the poor solubility of chitosan at elevated pH. The measured surface force profile was very similar to the one detected with the chitosan present in the bulk solution at pH ∼4, with the bridging attraction pulling the surfaces together from below of 11 nm into a separation of ∼1 nm. However, on separation, there was a notable decrease in the pull-off force that was measured to be 0.8 ± 0.3 mN/m. This is a consequence of the reduced charge density of the chitosan at the higher pH-value. The surface force profile was very similar when chitosan was first adsorbed outside of the SFA.

Effect of SDS on Chitosan Adsorption Layers, Low Ionic Strength. An addition of SDS to a concentration of 0.1 or 0.2 cmc SDS does not result in any measurable changes of the repulsive part of the force profile (Figure 6). This indicates that association of preadsorbed chitosan and SDS does not take place to any significant degree at this low SDS concentration.

A further increase in SDS concentration to 0.5 cmc (Figure 7) causes recharging of the surfaces.

As a result, a long-range slowly decaying repulsion develops that is measurable down to ∼4 nm. The slope of this force is slightly larger than expected for a pure double-layer force, see inset Figure 7. The likely reason for this is that a decrease in surface separation results in both a compression of the electrical double layer and a change to less extended conformations of the polymer chains as discussed in several theoretical works (see, e.g., refs 33−35). At shorter separations, the surface interactions are dominated by a stronger but more rapidly decaying steric repulsion due to compression of the compact part of the chitosan−SDS surface complexes. The thickness of the compressed layer is increased as compared to the thickness

TABLE 1. Adsorbed Amount of Chitosan on Mica after Exposure to the Solutions with Different SDS Concentrations Expressed as Number of Nitrogen Atoms, N, and Adsorbed Amount, Γ

	Al-mono		Al-elstat		Al-elstat (adjusted)	
SDS (cmc)	$N \times 10^{-18}$ (atoms/m^2)	Γ (mg/m^2)	$N \times 10^{-18}$ (atoms/m^2)	Γ (mg/m^2)	$N \times 10^{-18}$ (atoms/m^2)	Γ (mg/m^2)
			background 30 mM NaCl			
0	3.8−4.2	1.07−1.18	4.4−4.7	1.23−1.32	4.1−4.3	1.12−1.21
0.1	3.6−3.9	1.01−1.09	4.3−4.6	1.21−1.29	4.0−4.3	1.12−1.21
0.2	3.5−3.9	0.98−1.09	4.0−4.3	1.12−1.21	3.8−4.0	1.07−1.12
0.5	3.8−4.2	1.07−1.18	4.3−4.6	1.21−1.29	4.0−4.2	1.12−1.18
1.0	3.5−3.8	0.98−1.07	4.4−4.7	1.23−1.32	4.0−4.3	1.12−1.21
			background 0.1 mM NaCl			
0	3.1−3.4	0.87−0.95	3.6-3.9	1.01−1.09	3.4−3.6	0.95−1.09
0.1	3.2−3.5	0.90−0.98	3.6-3.9	1.01−1.09	3.4−3.7	0.95−1.09
0.2	2.6-2.9	0.73-0.81	3.7-4.0	1.04-1.12	3.4-3.6	0.95-1.12
0.5	2.7−3.0	0.76−0.84	3.7-3.9	1.04−1.09	3.4−3.6	0.95−1.09
1.0	2.6−2.9	0.73−0.81	3.8-4.1	1.07−1.15	3.5−3.7	0.98−1.15

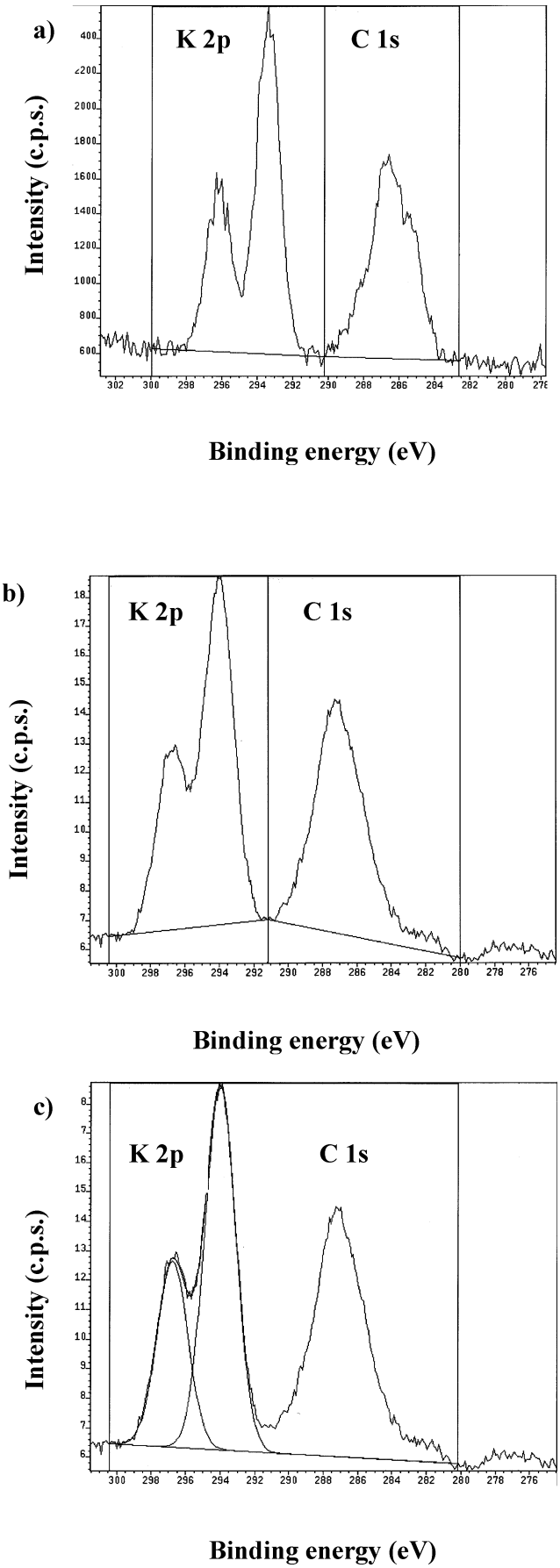

Figure 4. K 2p spectra for chitosan exposed to 0.5 cmc SDS solution in 30 mM NaCl. The spectra show also the C 1s peak at about 285−289 eV (a) Al-*mono* mode, (b) Al-*elstat* mode before adjustment of the baseline, and (c) Al-*elstat* mode after adjustment of the baseline.

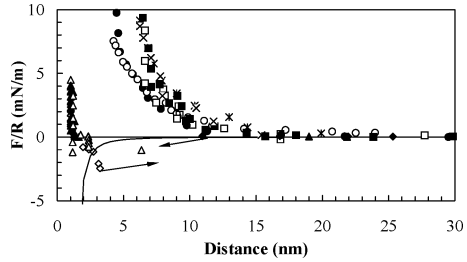

Figure 5. Force normalized by radius as a function of surface separation. The forces were measured between chitosan-coated surfaces across solutions of 0.1 mM $NaNO_3$ at pH ~4 (◆) and 6 (▲), solutions of 30 mM $NaNO_3$ at pH ~4 (●) and 6 (■) after adsorption outside of the SFA, and after dilution of the droplet inside of the SFA (∗). Filled symbols denote forces measured on approach, and open symbols show forces measured on separation. The arrows show inward and outward jumps. The solid line represents the expected van der Waals force assuming the Hamaker constant to be $A = 2 \times 10^{-20}$ (J).

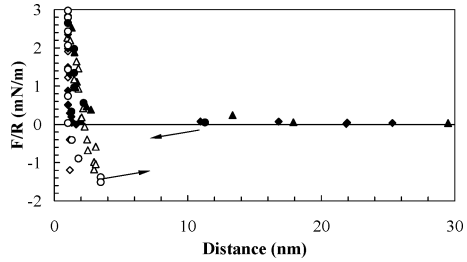

Figure 6. Force normalized by radius as a function of surface separation. Forces were measured between chitosan-coated surfaces in 0.1 mM $NaNO_3$ (◆) and across chitosan free solution containing 0.1 cmc SDS (●) and 0.2 cmc SDS (▲). Filled and unfilled symbols denote forces measured on approach and separation, respectively. The arrows indicate inward and outward jumps.

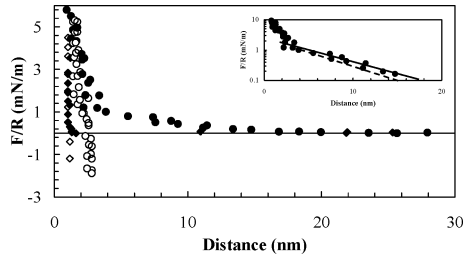

Figure 7. Force normalized by radius as a function of surface separation. Forces were measured between chitosan-coated surfaces in 0.1 mM $NaNO_3$ (◆) and across chitosan-free solution containing 0.5 cmc SDS (●). Filled symbols denote forces measured on approach and open symbols represent forces determined on separation. (Insert) The repulsive part of the force curve drawn on a logarithmic scale. The dashed line shows the slope of an electrical double-layer force at the given ionic strength. The solid line is drawn through the outer part on the experimentally measured force curve.

of the chitosan layer prior to SDS addition. The pull-off force is again increased as compared to the lower SDS concentrations.

An addition of SDS to a concentration of 1 cmc leads to a further increase in the magnitude of the slowly decaying component of the repulsion (Figure 8). The decay length of the outer part is very close to the one expected for a pure electrostatic double-layer force at the given electrolyte concentration, whereas a slower decay is noted below 6 nm. At very short separation, below 3 nm, the force remains steep.

It was also observed, after 1 h time, that the thickness of the compressed layer had increased significantly, indicating swelling. However, the compressed layer was markedly thinned after the chitosan-coated surfaces were allowed to stand for 20 h in 1 cmc SDS solution, suggesting that slow desorption of

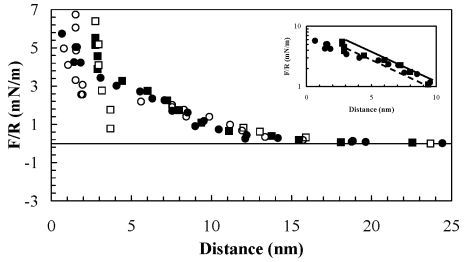

Figure 8. Force normalized by radius as a function of surface separation. Forces were measured between chitosan-coated surfaces across chitosan-free 0.1 mM $NaNO_3$ solution containing 1 cmc SDS after 1 (■) and 20 h (●) of exposure. Filled symbols denote forces encountered on approach, and open symbols represent forces detected on separation. (Insert) The repulsive part of the force curve drawn on a logarithmic scale. The dashed line corresponds to the theoretically calculated electrical double-layer force at the given ionic strength. The solid line is drawn through the outer part of the experimentally measured force curve.

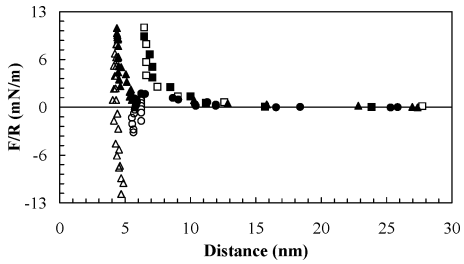

Figure 9. Interactions between mica surfaces coated with chitosan across solution containing 30 mM $NaNO_3$ (pH 6) in SDS-free solution (■), with 0.1 cmc (●), and with 0.2 cmc (▲) SDS added. Filled symbols denote forces measured on approach, and open symbols represent measurements on separation.

chitosan−SDS complex was taking place. (Note, this is not seen in the ESCA results due to the shorter desorption time, 1 h.) No attractive force was observed on separation at this SDS concentration.

Interactions in 30 mM $NaNO_3$. When chitosan was adsorbed from a solution containing 30 mM $NaNO_3$, the force−distance profile was dominated by a steric repulsion with a range of about 14−16 nm, thus yielding an undisturbed extended chitosan adsorption layer thickness of about 7−8 nm (Figure 5). Clearly, due to the screening of charges on the polyelectrolyte chain, in high ionic strength solutions the polyelectrolyte acquires a more curled conformation in the bulk and on the surface, thus leading to the thicker adsorption layers. Another notable feature of the surface interactions observed at high ionic strength was the absence of bridging attraction as well as a lack of hysteresis in the measured surface force curve. This suggests that the forces are measured under (quasi)equilibrium conditions, i.e., any conformational changes and adsorption/desorption processes occur rapidly or slowly compared to the experimental time scale (∼20 min).

The change in pH from ∼4 to 6 leads to swelling of the chitosan adsorption layer, but we could not find any evidence of desorption. The statement is based on the observations that the force profile was very similar at the two pH values and remained unchanged for at least 20 h after the pH change. It is also consistent with the data of Claesson and Ninham.[12]

Effect of SDS on Chitosan Adsorption Layers, High Ionic Strength. As can be seen from Figure 9, addition of SDS to a concentration of 0.1 cmc results in a slight collapse of the chitosan layers.

The magnitude of the long-range force is smaller and the compressed layer thickness is reduced when compared to the

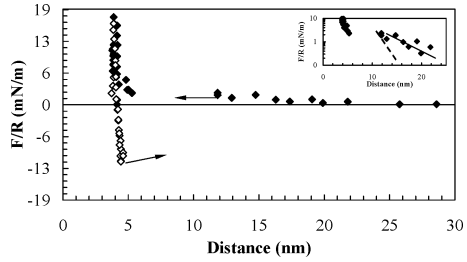

Figure 10. Interactions between mica surfaces coated with chitosan across solution containing 30 mM $NaNO_3$ (pH 6) with 0.5 cmc SDS added. Filled symbols show forces determined on approach, and open symbols represent forces detected on separation. The arrows show inward and outward jumps. (Insert) The repulsive part of the force curve drawn on a logarithmic scale. The dashed line corresponds to the theoretically calculated electrical double-layer force.

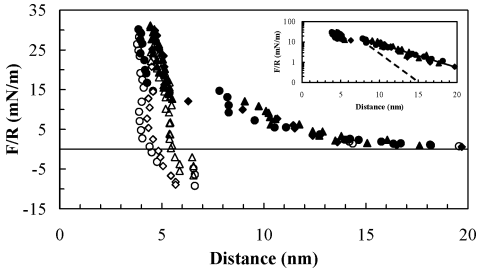

Figure 11. Interactions between mica surfaces coated with chitosan across solution containing 30 mM $NaNO_3$ and 1 cmc SDS. The measurements were performed 1 h after introducing SDS, first measurement (●), second measurement (◆). Measurement after 20 h of surface exposure to the solution of surfactant (▲). Solid symbols show data points obtained on approach, and open symbols denote data points acquired during separation. (Insert) The repulsive part of the force curve drawn on a logarithmic scale. The dashed line corresponds to the theoretically calculated electrical double-layer force at the given ionic strength, and the solid line is a fit through the data points.

SDS-free chitosan layer. Moreover, in contrast to the latter, the force curve is not purely repulsive but an attraction bringing the surfaces from a distance of below 9 nm to a separation of about 6 nm by a "jump in" is present. In accordance with this observation, on separation, a pull-off force of 2.6 ± 0.8 mN/m is detected.

An increase in SDS concentration to 0.2 cmc leads to further shrinkage of the chitosan adsorption layers (Figure 9). The jump brings the surfaces from below 10 to around 5 nm. By applying a higher compressive force the adsorption layers could be driven to a separation of 4 nm. The pull-off force required to separate the surfaces from this position was 11 ± 1 mN/m.

At 0.5 cmc SDS (Figure 10) the chitosan layer was collapsed even more than at the previous SDS concentration. We note that the ESCA results demonstrate that no desorption occurs due to SDS addition and the change in the surface interaction is thus clearly due to a collapse of the adsorbed layer and not due to a partial desorption.

The jump in was occurring from a separation of ca. 11 nm and brought the surfaces to 5 nm. Again, by increasing the compressive force the surfaces could be forced to a separation of just below 4 nm, where the pull-off force was 11 ± 1 mN/m. We also noted a weak long-range repulsive force. Just as at the lower electrolyte concentration, the decay length of this force is larger than expected for a pure double-layer force, and the mechanism is expected to be the same (Figure 10, insert).

Further increase of surfactant concentration to 1 cmc leads to some swelling of the chitosan layers and a reduction of the pull-off force (Figure 11).

We note that unlike the measurements carried out at low ionic strength and at 30 mM, at lower SDS concentrations the force profiles determined on subsequent measurements are not perfectly reproducible. This is a strong indication of a less rigid and slowly relaxing adsorbed polymer layer structure. The forces measured on the first approach were slightly less repulsive than those on the subsequent approach. Hence, the act of separating the surfaces has made the adsorbed layers less compact. The exposure of the adsorbed layer to the 1 cmc SDS solution for prolonged times (20 h) did not result in any notable force profile changes.

Discussion

We aim our discussion at the comparison of SDS interactions with, on one hand, chitosan, a hydrophilic and relatively stiff, weak polyelectrolyte, and, on the other hand, acryl amide-based polyelectrolyte, poly{2-(propionyloxy)ethyl}trimethylammonium chloride (PCMA), which possesses a weakly hydrophobic backbone, is more flexible, and carries a permanent positive charge. This polyelectrolyte was extensively studied by Claesson et al.[13,36−38]

Association of Chitosan and SDS in Bulk. Association of SDS and cationic polyelectrolytes is partly driven by electrostatic attraction between the opposite charges. The importance of the ionic component of the chitosan−SDS interactions was clearly demonstrated by Wey and Hudson,[39] who showed, by measuring binding isotherms, that an increase in concentration of added salt results in a shift of the binding region to higher free surfactant concentrations. The turbidity studies of chitosan−SDS mixtures (Figure 1) shows that the behavior of the formed aggregates is different from that observed for PCMA−SDS. The first thing that stands out from the comparison of the turbidity curves for the two polyelectrolytes (Figure 1 and ref 37) is the fact that chitosan−SDS complexes show only a weak tendency for redispersion at the elevated SDS concentrations. In contrast, in a solution of PCMA−SDS at 1 cmc SDS, the redissolution was close to complete due to repulsion between recharged polyelectrolyte−surfactant complexes as indicated by a strong decrease in turbidity at SDS concentrations occurring already above 0.1 cmc. One may suggest that in the chitosan−SDS system only limited recharging occurs and the surfactant binding ceases close to the charge neutralization condition. However, to prove this point, electrokinetic data showing mobility of the chitosan−SDS aggregates are required which at present are not available. Another notable feature of the chitosan−SDS aggregates pinpointing the structural differences as compared to PCMA−SDS aggregates is the appearance of the flocks and their sediment. While PCMA−SDS aggregates seem to be very compact and the sediments are not easily redispersible, the chitosan−SDS aggregates are soft and loose and can be easily redispersed once sedimented. It was demonstrated by small-angle X-ray scattering (SAXS)[40] that the internal structure in PCMA−SDS aggregates is hexagonal whereas a polyelectrolyte without side chains, poly(vinylamine), mixed with SDS forms a lamellar structure. Babak et al. achieved an ordered nanostructure in a complex formed between chitosan and SDS by interfacial diffusion in a water−water emulsion.[41,42] This complex included chitosan and SDS micelles that cross-linked the cationic polymer chains. The SAXS studies of this system[42] were also indicative of the formation of fragments with a lamellar structure. With the above in mind, we can speculate that the internal structure of our chitosan−SDS aggregates will be similar to that found by Babak et al. Some indication for the formation of an ordered structure in chitosan−SDS complex at the solid−liquid interface is also present in our surface force data (Figure 12).

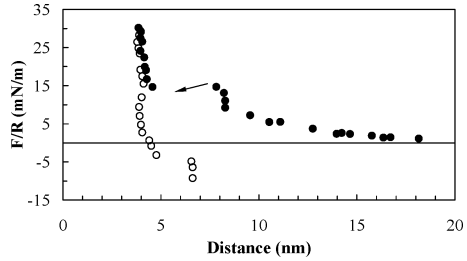

Figure 12. Interactions between mica surfaces coated with chitosan across solution containing 30 mM $NaNO_3$ and 1 cmc SDS. The measurements were performed 1 h after introducing SDS. The arrow indicates an inward jump.

As clearly seen from Figure 12, on approach an inward jump of ∼4 nm occurs. This jump is comparable to the cross-section of SDS−bilayer aggregates, disregarding the surrounding ionic cloud, and similar to that observed for the PCMA−SDS system using surface force, SANS and SAXS measurements.[40] The structuring in the chitosan−SDS complexes adsorbed on mica is significantly less expressed compared to what was observed previously in adsorbed PCMA−SDS complexes,[13,36] which once again points to a different structural arrangement in the two polyelectrolyte−SDS systems.

Chitosan at a Solid−Liquid Interface: Effect of Ionic Strength and SDS. Adsorption of chitosan on mica surfaces is largely dependent on the ionic strength of the solution. As evidenced by the chemical surface analysis (Table 1), the adsorbed amount of chitosan is ∼20% larger from 30 mM than from 0.1 mM NaCl. Furthermore, the SFA data (Figure 5) demonstrate that considerably thicker adsorption layers are obtained at elevated salt concentrations. We note that the thickness increase is ∼80%, considerably more than the increase in the adsorbed amount. Hence, it is clear that the adsorbed layer of chitosan obtained at higher ionic strength contains significantly more water than that obtained at low salt concentration.

The way the oppositely charged surfactant interacts with the preadsorbed polyelectrolyte is, to a large extent, determined by the background salt concentration. While in solution binding of the surfactant to a polyelectrolyte is counteracted by increasing the ionic strength of the solution,[39] at the negatively charged surface the very opposite is observed. Comparison of Figures 6 and 9 clearly illustrates this point. While at low ionic strength the addition of SDS up to 0.2 cmc does not have any significant effect, at 30 mM $NaNO_3$ it causes the collapse of the adsorbed layer and a significant increase in the pull-off force due to the incorporation of SDS. This is due to the resulting decrease in net charge and hydrophobic interactions between the surfactant tails. The opposite trends of SDS−cationic polymer interactions in bulk and at the negatively charged surface can be rationalized considering the role of the surface. As can be understood from the very thin (∼0.5 nm) adsorbed chitosan layer on the mica surface (Figure 5), there is a near-to-perfect match between the negative mica lattice sites and the positive charges of chitosan. In this situation the surface is a strong competitor to the surfactant, and thus, the binding of the surfactant to the polyelectrolyte is hindered. In the presence of a higher amount of salt, due to electrostatic screening, the polyelectrolyte adopts a significantly more extended conformation on the surface. The presence of loops and tails makes the initial binding of SDS to the positive sites of the polyelectrolyte easier.

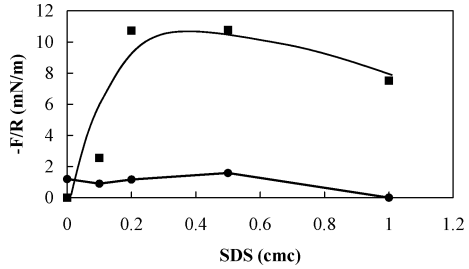

Figure 13. Pull-off force as a function of SDS concentration in 30 mM (■) and in 0.1 mM $NaNO_3$ (●).

It is of some interest to take a closer look at the issue of pull-off force variations with SDS concentration at the two different salt concentrations (Figure 13).

As seen from Figure 13, at high levels of salt there is a very steep increase in the pull-off force with the amount of SDS up to 0.2 cmc. Above this concentration the pull-off force levels off and slightly decreases at about 1 cmc SDS. In low ionic strength solutions the pull-off force increases only marginally at intermediate SDS concentrations and finally drops to 0 at 1 cmc SDS. Looking back at the two sets of force data (Figures 5−8, low ionic strength, and Figures 5 and 9−11, high ionic strength) it is clear that there exists a very delicate balance between the forces involved in the surface−polyelectrolyte−SDS−salt system. At low ionic strength, the contact between the surface and adsorbed polyelectrolyte is extremely intimate. This hinders the association of the surfactant with the pre-adsorbed polymer at low surfactant concentrations. At 0.5 cmc the concentration of the surfactant is increased enough for the association to occur. As seen from Figures 7 and 13, as a result both a recharging of the adsorbed layer occurs and the pull-off force increases due to SDS interlayer bridges. There is a clear balancing between the repulsive electrical double-layer force and attraction due to the hydrophobic interactions. At higher salt concentration, where the contact of the polymer and the surface is less close, the binding of the SDS occurs, as discussed above, more readily. Therefore, a significantly larger number of surfactant-mediated bridges can form, which is clearly seen from the magnitude of the pull-off force (Figure 13). The bridging due to the SDS-mediated intersurface links is strong enough to be considerable even at such a high SDS concentration as 1 cmc, though some reduction of the magnitude of this force does take place.

Conclusions

The weak (pK_a 6.6) cationic polymer, chitosan, readily adsorbs on negatively charged mica surfaces from low and high ionic strengths solutions. Larger adsorbed amounts and considerably thicker adsorbed layers are obtained when adsorption occurs at the elevated ionic strength. Adsorption from higher ionic strength solutions leads to less intimate contact between the surface and the polyelectrolyte as compared to adsorption from low ionic strength solutions. Hence, the interaction between the polymer and the surfactant at the surface is facilitated in the presence of elevated salt amounts. This is in contrast to the bulk association process. As shown by the ESCA results, no detectable desorption of chitosan from mica surfaces is attained during the short (1 h) surface exposure times to the solutions of SDS even at high SDS concentrations, regardless of the ionic strength of the solution. This pinpoints chitosan as a possible polymer for surface coatings where exposure of the surfaces to surfactants is required. The association of SDS with the chitosan at the surface leads to the hydrophobic domain formation. In the 30 mM salt solution, this results in a compacting of the adsorbed layer. Upon contact between such SDS-loaded surfaces, a strong surface adhesion develops which is able to counteract the electrical double-layer repulsion even at elevated SDS concentrations.

Acknowledgment. A.D. acknowledges financial support of Marie Curie Postdoctoral Fellowship within FP5.

References and Notes

(1) Ravi Kumar, M. N. V. *React. Funct. Polym.* **2000**, *46*, 1.
(2) Coma, V.; Martial-Gros, A.; Garreau, S.; Copinet, A.; Salin, F.; Deschamps, A. *J. Food Sci.* **2002**, *67*, 1162.
(3) Felse, P. A.; Panda, T. *Bioprocess Eng.* **1999**, *20*, 505.
(4) Xie, W. M.; Xu, P. X.; Wang, W.; Liu, Q. *Carbohydr. Polym.* **2002**, *50*, 35.
(5) Xie, W. M.; Xu, P. X.; Wang, W.; Liu, Q. *J. Appl. Polym. Sci.* **2002**, *85*, 1357.
(6) Muzzarelli, R. A. A.; Muzzarelli, C.; Tarsi, R.; Miliani, M.; Gabbanelli, F.; Cartolari, M. *Biomacromolecules* **2001**, *2*, 165.
(7) Tarsi, R.; Muzzarelli, R. A. A.; Pruzzo, C.; Pruzzo, C. *J. Dent. Res.* **1997**, *76*, 665.
(8) Tarsi, R.; Corbin, B.; Pruzzo, C.; Muzzarelli, R. A. A. *Oral Microbiol. Immunol.* **1998**, *13*, 217.
(9) Domard, A.; Rinaudo, M.; Terrassin, C. *J. Appl. Polym. Sci.* **1989**, *38*, 1799.
(10) Fält, P.; Bergenståhl, B.; Claesson, P. M. *Colloids Surf., A* **1993**, *71*, 187.
(11) Holmberg, M.; Berg, J.; Stemme, S. S.; Ödberg, L.; Rasmusson, J.; Claesson, P. M. *J. Colloid Interface Sci.* **1997**, *186*, 369.
(12) Claesson, P. M.; Ninham, B. W. *Langmuir* **1992**, *8*, 1406.
(13) Claesson, P. M.; Dedinaite, A.; Blomberg, E.; Sergeyev, V. G. *Ber. Bunsen-Ges. Phys. Chem.* **1996**, *100*, 1008.
(14) Fielden, M. L.; Claesson, P. M.; Schillen, K. *Langmuir* **1998**, *14*, 5366.
(15) Claesson, P. M.; Fielden, M. L.; Dedinaite, A. *J. Phys. Chem. B* **1998**, *102*, 1270.
(16) Rojas, O. J.; Neuman, R. D.; Claesson, P. M. *J. Colloid Interface Sci.* **2001**, *237*, 104.
(17) Rojas, O. J.; Ernstsson, M.; Neuman, R. D.; Claesson, M. P. *Langmuir* **2002**, *18*, 1604.
(18) Plunkett, M. A.; Claesson, P. M.; Rutland, M. W. *Langmuir* **2002**, *18*, 1274−1280.
(19) Rojas, O. J.; Ernstsson, M.; Neuman, R. D.; Claesson, P. M. *J. Phys. Chem. B* **2000**, *104*, 10032.
(20) Parker, J. L.; Christenson, H. K.; Ninham, B. W. *Rev. Sci. Instrum.* **1989**, *60*, 3135.
(21) Israelachvili, J. N.; Adams, G. E. *J. Chem. Soc., Faraday Trans. 1* **1978**, *74*, 975.
(22) Israelachvili, J. N. *J. Colloid Interface Sci.* **1973**, *44*, 259.
(23) Derjaguin, B. *Kolloid. Z.* **1934**, *69*, 155.
(24) Parker, J. L.; Attard, P. J. *J. Phys. Chem.* **1992**, *96*, 10398.
(25) Wagner, C. D. *Anal. Chem.* **1977**, *49*, 1282.
(26) Vandensteeg, H. G. M.; Stuart, M. A. C.; Dekeizer, A.; Bijsterbosh, B. H. *Langmuir* **1992**, *8*, 2538.
(27) Linse, P. *Macromolecules* **1996**, *29*, 326.
(28) Dahlgren, M. A.; Waltermo, A.; Blomberg, E.; Claesson, P. M.; Sjostrom, L.; Akesson, T.; Jonsson, B. *J. Phys. Chem.* **1993**, *97*, 11769.
(29) Dahlgren, M. A.; Claesson, P. M.; Audebert, R. *J. Colloid Interface Sci.* **1994**, *166*, 343.
(30) Strand, S. P.; Vandvik, M. S.; Vårum, K. M.; Östgaard, K. *Biomacromolecules* **2001**, *2*, 126.
(31) Anthonsen, M. W.; Smidsröd, O. *Carbohydr. Polym.* **1995**, *26*, 303.
(32) Strand, S. P.; Tömmeraas, K.; Värum, K. M.; Östgaard, K. *Biomacromolecules* **2001**, *2*, 1310.
(33) Mikalvic, S. J.; Marcelja, S. *J. Phys. Chem.* **1988**, *92*, 6718.
(34) Pincus, P. *Macromolecules* **1991**, *24*, 2912.
(35) Zhulina, E. B.; Borisov, O. V.; Birshtein, T. M. *Macromolecules* **2000**, *33*.
(36) Dedinaite, A.; Claesson, M. P.; Bergström, M. *Langmuir* **2000**, *16*, 5257.
(37) Dedinaite, A.; Claesson, P. M. *Langmuir* **2000**, *16*, 1951.
(38) Claesson, P. M.; Bergström, M.; Dedinaite, A.; Kjellin, M.; Legrand, J.-F.; Grillo, I. *J. Phys. Chem. B* **2000**, *104*, 11689.
(39) Wei, Y. C.; Hudson, S. M. *Macromolecules* **1993**, *26*, 4151.
(40) Bergström, M.; Kjellin, U. R. M.; Claesson, M. P.; Pedersen, J. S.; Nielsen, M. M. *J. Phys. Chem. B* **2002**, *106*, 11412.
(41) Babak, V. G.; Merkovich, E. A.; Desbrieres, J.; Rinaudo, M. *Polym. Bull.* **2000**, *45*, 77.
(42) Babak, V. G.; Merkovich, E. A.; Galbraikh, L. S.; Shytkova, E. V.; Rinaudo, M. *Mendeleev Commun.* **2000**, 94.